Erzincan Üniversitesi
Fen Bilimleri Enstitüsü Dergisi
2021, 14(2), 517-523
ISSN: 1307-9085, e-ISSN: 2149-4584
Araştırma Makalesi

Erzincan University
Journal of Science and Technology
2021, 14(2), 517-523
DOI: 10.18185/erzifbed.945118
Research Article

X-ray Properties of *Spitzer*/IRAC Selected AGNs

Tuba İkiz[1,2]

[1]Department of Astronomy and Space Sciences, Faculty of Science, Atatürk University, Erzurum, Turkey
[2] Atatürk University Astrophysics Research and Application Center (ATASAM), Erzurum, Turkey

Geliş / Received: 30/05/2021, Kabul / Accepted: 04/07/2021

Abstract
Spitzer/IRAC color selection is a powerful tool to identify hot accreting nuclei, that is to say AGN, in galaxies. In this study, mid-infrared detected candidate 36 AGNs are used that are selected from the *Spitzer* Survey of Stellar Structures in Galaxies (S^{4}G) sample consisting of more than 2500 galaxies together with its extension sample of more than 400 galaxies by İkiz et al., (2020). Mid-infrared color selection method is tested by examining the X-ray properties of the galaxies via the *XMM-Newton* and *Chandra*. Using the X-ray data, we demonstrate that galaxies displaying hot mid-infrared nuclei stand out as (candidate) active galaxies. 64% of mid-infrared-selected AGN are detected at X-ray energies in *XMM-Newton* and *Chandra* data. It has been hypothesized that IRAC sources with AGN colors that lack X-ray detections are predominantly high-luminosity AGN that are obscure.

Key words: galaxies: active – galaxies: nuclei – infrared: galaxies – X-rays: galaxies

Spitzer/IRAC Seçilmiş AGN'lerin X-ışın Özellikleri

Öz
Spitzer/IRAC renk seçimi, galaksilerdeki sıcak madde biriktiren çekirdekleri, bir başka ifadeyle AGN'i tanımlamak için güçlü bir araçtır. Bu çalışmada İkiz et al., (2020) tarafından 2500'den fazla galaksiden oluşan Galaksilerdeki Yıldız Yapılarının *Spitzer* Araştırması (S^{4}G) örneklemesine ek olarak onun uzantısı 400 galaksiden oluşan örneklemeden orta-kırmızı öte renk seçim yöntemi ile seçilmiş 36 AGN kullanılmıştır. Kırmızı ötesi renk seçimi yöntemi, *XMM-Newton* ve *Chandra* verileri ile galaksilerin X-ışını özellikleri incelenerek test edilmiştir. X-ışını verilerini kullanarak, sıcak orta kırmızı ötesi çekirdek sergileyen galaksilerin (aday) aktif galaksiler olarak öne çıktığı gösterilmiştir. Orta-kırmızı ötesi seçilmiş AGN'lerin %64'ü *XMM-Newton* ve *Chandra* verilerinde X-ışını enerjilerinde tespit edilmiştir. X-ışını tespitleri olmayan AGN renklerine sahip IRAC kaynakların büyük çoğunluğunun yüksek ışıtmalı örtülmüş AGN'ler olduğu varsayılmıştır.

Anahtar Kelimeler: galaksiler: aktif - galaksiler: çekirdekler - kırmızı öte: galaksiler - X-ışınları: galaksiler

1. Introduction

Galaxies are known to contain supermassive black holes (e.g., Ferrarese and Merritt, 2000) in their centers, whose masses correlate with the masses of their bulges, indicating that the processes of forming bulges and supermassive black holes are intimately related (Magorrian

*Corresponding Author: tubaaaikiz@gmail.com

et al., 1998; Tremaine et al., 2002). These supermassive black holes reside in all massive galaxies and growth and evolution of galaxies is closely linked to the growth and evolution of the supermassive black holes (e.g., Kauffmann and Haehnelt, 2000; Heckman, 2008). A small fraction of galaxies also has a very bright nucleus called an Active Galactic Nucleus (AGN), showing excess emission due to accretion of mass by the supermassive black hole that situates at the center of the galaxy. It is thought that AGN plays a dominant role during the formation of galaxies by creating large outflows that quench star formation in the galaxy (Kormendy and Ho, 2013). The nucleus of active and inactive galaxies are thus an ideal laboratory for studying the evolution and formation of galaxies. AGNs are among the most luminous objects in the universe and identifying these objects in all states of accretion and obscuration and accurately understanding their properties and structure is a key step to understand how galaxies evolve with cosmic time. Recent theoretical work suggests that feedback from AGN plays a significant role in establishing the present-day appearances of galaxies (e.g., Silk and Rees, 1998; Hopkins et al., 2008).

AGN can be defined in several ways at essentially all wavelengths (mid-infrared, X-rays, and radio detections and optical emission line diagnostics). Selection of AGN in the mid-infrared allows the exploration of strong AGN and quasars whose optical and soft X-ray emission is hidden by dust (e.g. Lacy et al., 2004, 2007, 2015; Stern et al., 2005; Martínez-Sansigre et al., 2005; Stern et al., 2012; Donley et al., 2012; Eisenhardt et al., 2012; İkiz et al., 2020). High-energy radiation from the AGN is reprocessed by dust near the AGN and reradiated at mid-infrared wavelengths. Luminous AGNs show a red mid-infrared power-law spectral energy distribution (SED), which is dominated by thermal emission from hot dust (Neugebauer et al., 1979; Elvis et al., 1994; Rieke and Lebofsky, 1981). Mid-infrared identification is sensitive to both obscured and unobscured AGNs, without requiring deep X-ray survey data. Emission at mid-infrared wavelengths can also possibly be used to detect Compton-thick AGNs that may be unnoticed by deep X-ray surveys (e.g. Ivison et al., 2004; Lacy et al., 2004; Stern et al., 2005; Alonso-Herrero et al., 2006; Polletta et al., 2006).

The presence of an extremely hot accretion disk in combination with a surrounding molecular torus, AGNs can be studied across the entire electromagnetic spectrum. The central region produces large amounts of X-rays which heat and ionize the surrounding gas and dust. Their X-ray continuum can be detected by X-ray satellites. Their emission may be weakened or blocked completely depending on the gas column density along the line of sight. The hard (2-10 keV) X-ray and mid-infrared wavebands provide powerful, complementary methods for identifying and studying AGN over a wide range of intrinsic obscuration (Eckart et al., 2018).

2. Material and Methods

Spitzer Space Telescope is a powerful tool for studying AGN demographics. In this study we used the *Spitzer* Survey of Stellar Structures in Galaxies (S^4G; Sheth et al., 2010) AGNs that are detected by infrared excess method by İkiz et al., (2020). They showed that this method is one of the best ways of distinguishing AGNs from normal galaxies and an efficient way of finding AGNs in a large sample. The S^4G is a volume, magnitude, and size-limited survey of more than 2500 nearby galaxies using the IRAC Infrared Array Camera (Fazio et al., 2004) with deep imaging at 3.6 and 4.5 μm on board the *Spitzer* Space Telescope which one of the *Spitzer* Legacy Programs of late type galaxies. This survey contains galaxies within 40 Mpc (v<3000 km/s), away from the galactic plane (|b| >30°), with extinction corrected B-band magnitude brighter than 15.5 and B-band diameter larger than 1' with distances determined from HI radial velocities. The S^4G sample had been expanded with new S^4G Extension observations for elliptical galaxies. Because galaxies need to contain HI many ellipticals are not included in the original S^{4}G sample, and therefore the observations for the S^{4}G Extension sample were taken. In İkiz et al., (2020) study, 2741 S^{4}G sample galaxies are analyzed using mid-infrared excess method and 36 galaxies are detected candidate AGNs with searching counterparts in the Faint Images of the Radio Sky at Twenty-Centimeters (FIRST) and the National Radio Astronomical Observatory VLA Sky Survey (NVSS) survey catalogues. In this study 36 S^{4}G AGNs are examined in *XMM-Newton* and *Chandra* survey catalogues to detect X-ray counterparts. All compact X-ray sources with a luminosity above ≈ 10^{42} erg s^{-1}(2-10 keV) are considered to be AGN. Because of the broad wavelength coverage of the X-ray band, there is a remarkable difference between the soft-band (0.2-2 keV), the hard-band (2-6 keV) and the very hard-band (5-10 keV) surveys. The soft X-ray selection applicatively finds broad-line quasars and narrow line Seyfert galaxies (these objects tend to have a bright, soft spectral component, in addition to a flat, high energy, power-law spectrum). The hard X-ray selection finds, in addition to classical Seyfert 1 galaxies and quasars, large numbers of objects with weak or absent optical emission lines and lacking non-thermal nuclei. X-ray surveys with *XMM-Newton* and *Chandra* at energies < 10 keV are sensitive to all but the most heavily obscured AGN.

3. Results and Discussion

S^{4}G survey infrared detected candidate AGNs are examined in the archives of X-ray surveys. *XMM-Newton* has a large field of view of 30″ it provides a rich resource for serendipitous data thus providing a major resource, a deep, large-area sky survey. In the 3XMM-DR5 catalogue, the detection is considered as an extended source (Rosen et al., 2016). The *Chandra* Source Catalog (CSC) 1.1 release includes point and compact sources with observed spatial extents <~30″ (Evans et al. 2010). In this study, AGN candidate counterparts are identified in 3XMM-DR5 and *Chandra* catalogues within 30″. The 36 AGNs are listed in Table 2; well-known Seyfert galaxies NGC 1068, NGC 4051, and NGC 4151 are clearly detected.

64% of S^{4}G galaxies are detected in X-ray surveys as a hot-core (AGN candidate). Our detection statistics are not as high as optical spectroscopic surveys, but using the mid-infrared selection method with X-ray comparison is also effective to find AGN. In comparison with the study of İkiz et al., (2020) although the X-ray core detection is not as much as radio detection (88 %), it has enabled the counterparts of a large majority of AGNs. In addition, NGC 0625, NGC 7552 and NGC 7582 galaxies were detected in X-ray survey data, while they could not be detected in radio survey data.

Table 1. Fractions and numbers of hot- and cold-core galaxies detected in the two X-ray surveys

Survey	**Fraction**	**Hot-core (S^{4}G)**
X-ray	63.9 ± 8.0	23/36
XMM-Newton	58.3 ± 8.2	21/36
Chandra	36.1 ± 8.0	13/36
Survey	**Fraction**	**Cold-core (S^{4}G)**
X-ray	14.9 ± 0.7	402/2705
XMM-Newton	10.8 ± 0.6	292/2705
Chandra	10.1 ± 0.6	227/2705

Notes. The hot-core galaxies are the *Spitzer*-detected AGN detected in the X-ray, while the cold-core galaxies are only detected in the X-ray and not as infrared-detected AGN.

Table 2. Detection of Spitzer selected AGNs in two X-ray surveys.

Galaxy (1)	**RA** (deg) **(2)**	**DEC** (deg) **(3)**	**TT** (4)	**[3.6]-[4.5]** (mag) **(5)**	**Error** (mag) **(6)**	**X-ray (Detected/ Non-detected) (7)**	**Survey (*XMM-Newton, Chandra*) (8)**
ESO 409-015	1.38364	-28.09991	5.4	0.800	0.413	**Non-detected**	-
NGC 0253	11.86515	-31.42178	-1.2	0.789	0.021	**Non-detected**	-
NGC 0520	21.14538	3.79159	1.3	0.522	0.043	Detected	*XMM-Newton,Chandra*
NGC 0625	23.76455	-41.43722	9.0	0.688	0.137	Detected	*XMM-Newton,Chandra*
NGC 0660	25.75969	13.64581	1.3	0.568	0.026	Detected	*XMM-Newton,Chandra*
NGC 0814	32.65672	-15.77344	-1.7	0.744	0.108	**Non-detected**	-
PGC 009354	36.88651	-10.16587	5.1	0.843	0.199	**Non-detected**	-
NGC 1068	40.66962	-0.01331	3.0	0.797	0.017	Detected	*XMM-Newton,Chandra*
NGC 1365	53.40155	-36.14039	3.2	0.679	0.020	Detected	*XMM-Newton*
IC 1953	53.42431	-21.47868	6.2	0.989	0.150	**Non-detected**	-
NGC 1386	54.19239	-35.99920	-0.7	0.783	0.033	Detected	*XMM-Newton,Chandra*
NGC 3034	148.96800	69.67975	7.5	0.690	0.013	Detected	*XMM-Newton*
NGC 3094	150.35812	15.77011	1.1	0.950	0.028	Detected	*XMM-Newton*
NGC 3227	155.87740	19.86513	1.5	0.590	0.026	Detected	*XMM-Newton*
NGC 3516	166.69780	72.56850	-2.0	0.519	0.035	Detected	*XMM-Newton*
UGC 06433	171.38258	38.06064	9.2	0.834	0.308	**Non-detected**	-
NGC 3729	173.45578	53.12555	1.2	0.704	0.067	**Non-detected**	-
NGC 4051	180.79007	44.53131	4.0	0.748	0.030	Detected	*XMM-Newton*
NGC 4151	182.63561	39.40578	2.0	0.988	0.029	Detected	*XMM-Newton,Chandra*
NGC 4293	185.30347	18.38261	0.3	0.635	0.048	**Non-detected**	-
NGC 4388	186.44490	12.66209	2.8	0.855	0.033	Detected	*XMM-Newton,Chandra*
NGC 4355	186.72764	-0.87767	1.1	1.358	0.066	Detected	*Chandra*
NGC 4593	189.91437	-5.34414	3.0	0.667	0.035	Detected	*XMM-Newton*
NGC 4628	190.60520	-6.97103	2.9	0.812	0.045	**Non-detected**	-
ESO 443-042	195.87400	-29.82870	3.0	0.597	0.091	**Non-detected**	-
NGC 4968	196.77420	-23.67690	-2.0	0.744	0.045	Detected	*XMM-Newton*
NGC 5253	204.98315	-31.64006	8.9	1.298	0.027	Detected	*XMM-Newton*
NGC 5347	208.32421	33.49085	2.0	0.890	0.044	Detected	*Chandra*
NGC 5427	210.85854	-6.03075	5.0	0.506	0.082	**Non-detected**	-
NGC 5506	213.31209	-3.20757	1.2	1.059	0.029	Detected	*XMM-Newton,Chandra*
NGC 5861	227.31709	-11.32171	5.0	1.601	0.084	**Non-detected**	-
NGC 7314	338.94252	-26.05043	4.0	0.712	0.047	Detected	XMM-Newton,Chandra
NGC 7378	341.94867	-11.81664	2.2	0.803	0.072	**Non-detected**	-
NGC 7479	346.23590	12.32293	4.3	1.150	0.041	Detected	*XMM-Newton*
NGC 7552	349.04494	-42.58496	2.4	0.511	0.028	Detected	*XMM-Newton,Chandra*
NGC 7582	349.59837	-42.37034	2.1	0.890	0.026	Detected	*XMM-Newton,Chandra*

Notes. Columns are: (1) Galaxy name; (2) Right ascension (J2000); (3) Declination (J2000); (4) Numerical morphological type; (5) [3.6]-[4.5] color (İkiz et al. 2020); (6) [3.6]-[4.5] color error (İkiz et al. 2020); (7) X-ray (Detected/Non-detected); (8) Survey. Column (7) indicates whether AGN detected or non-detected in both surveys. Column (8) refers to whether AGN are detected in the archives of *XMM-Newton* and *Chandra* within 30″ radius, respectively. (–) refers to the lack of data in both surveys.

Table 2 shows that about 36% (13 out of 36) of the infrared-detected candidate AGN have never before been detected as AGN in X-ray surveys. The two individual X-ray surveys are illustrated in the histograms of Figure 1. This figure shows that *XMM-Newton* survey detection is more sensitive than *Chandra* to find hot-core candidate AGN. It was determined that ESO 409-015, NGC 0253, UGC 06433 and NGC 7378 galaxies are defined as non-detected AGNs in both X-ray surveys mentioned in this study and also radio surveys refers in İkiz et al., (2020) study.

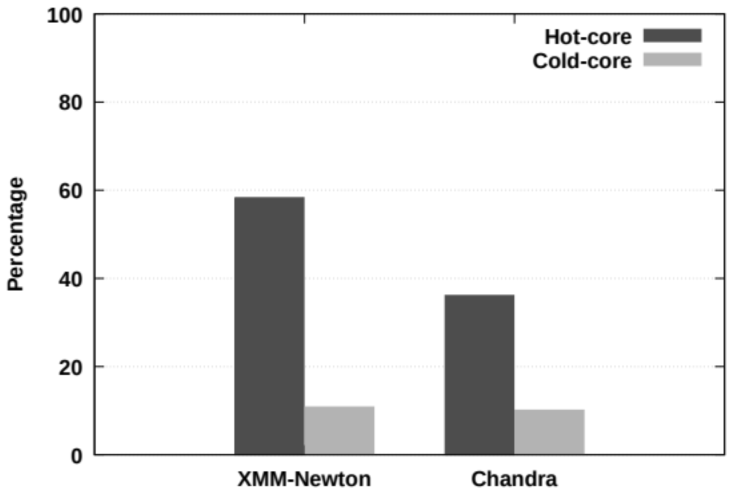

Figure 1. The fraction of Spitzer detected candidate AGN also detected in other surveys for *XMM-Newton* and *Chandra* (in dark colors in the histogram). Light colors in the histogram refer to the candidate non-AGN.

4. Conclusion

X-ray selection is one of the ways of finding active galaxies. It has been known over 40 years that the great majority of high latitude, point-like “hard” X-ray sources are AGN. Like radio emission, luminous, compact X-ray emission is almost a certain identifier of the existence of an AGN and does not need “confirmation” by data in other wavelength bands (Mushotzky, 2004). X-ray emission originates from very close to the central black hole, often showing large amplitude, rapid variability, and being characterized by a non-thermal spectrum (Mushotzky et al., 1993). Thus the X-ray properties are directly connected to the black hole nature of the AGN and are not due to reprocessing of the radiation.

XMM-Newton and *Chandra* are very sensitive to the presence of AGN. Sources in the luminosity range 10^{42}-10^{46}erg s^{-1} can be detected out to z∼3, independent of the nature of the host galaxy (Steffen et al., 2003). In the low redshift universe, there are no galaxies with an aggregate (non-AGN) luminosity exceeding this level. Thus, even without detailed X-ray spectra or imaging, the identification of the nature of the source is clear. As such, IRAC selection is a powerful technique not only for detecting heavily obscured AGNs missed in the X-ray, but also selecting luminous obscured and unobscured AGNs when deep X-ray data are absent. These results show that 2-10 keV X-ray surveys are efficient at finding candidate AGN sources missed by mid-infrared selection techniques. Many of the X-ray undetected *Spitzer* AGN are heavily obscured, resulting in faint optical counterparts and X-ray non-detection.

References

Alonso-Herrero, A. et al. 2006. Infrared Power-Law Galaxies in The Chandra Deep Field–South: Active Galactic Nuclei and Ultraluminous Infrared Galaxies, The Astrophysical Journal, 640:167–184.

Della Ceca R., et al., 2008. The Cosmological Properties of AGN in The XMM-Newton Hard Bright Survey, Astronomy & Astrophysics, 487, 119–130.

Donley, J. L., Koekemoer, A. M., Brusa, M., et al. 2012. Identifying Luminous Active Galactic Nuclei in Deep Surveys: Revised IRAC Selection Criteria, The Astrophysical Journal, 748:142.

Eckart, A., M. Zajacek, M. Parsa, et al. 2018. The Multifrequency Behavior of Sagittarius A*, Proceedings of Science, ArXiv:1806.00284.

Elvis M. et al., 1994. Atlas of Quasar Energy Distributions, The Astrophysical Journal Supplement Series, 95:1-68.

Evans I. N., et al., 2010. The Chandra Source Catalog, The Astrophysical Journal Supplement Series, 189:37–82.

Fazio, G. G., Hora, J. L., Allen, L. E., et al. 2004. The Infrared Array Camera (IRAC) For The Spitzer Space Telescope, The Astrophysical Journal Supplement Series, 154:10–17.

Ferrarese, L. & Merritt, D. 2000. A Fundamental Relation Between Supermassive Black Holes and Their Host Galaxies, The Astrophysical Journal, 539: L9–L12.

Heckman, T. M. 2008. The Escape Fraction of Ionizing Photons from High Redshift Galaxies from Data-constrained Reionization Models, Monthly Notices of the Royal Astronomical Society, ArXiv:1207.3803v2.

Hopkins, P. F., Hernquist, L., Cox, T. J., and Kereš, D. 2008. A Cosmological Framework for The Co-Evolution of Quasars, Supermassive Black Holes, And Elliptical Galaxies. I. Galaxy Mergers and Quasar Activity, The Astrophysical Journal Supplement Series, 175:356-389.

İkiz, T., Peletier, R.F., Barthel, P., et al. 2020. Infrared-detected AGNs in The Local Universe, Astronomy & Astrophysics, 640, A68.

Ivison, R. J., et al. 2004. Spitzer Observations of Mambo Galaxies: Weeding Out Active Nuclei in Starbursting Protoellipticals, The Astrophysical Journal Supplement Series, 154:124–12.

Kauffmann G. Haehnelt M., 2000. A Unified Model for The Evolution of Galaxies and Quasars Monthly Notices of the Royal Astronomical Society, 311, 576-588.

Kormendy, J. & Ho, L. C. 2013. Coevolution (Or Not) Of Supermassive Black Holes and Host Galaxies: Supplemental Material, ArXiv:1308.6483.

Lacy, M., Petric, A. O., Sajina, A., et al. 2007. Optical Spectroscopy and X-Ray Detections of a Sample of Quasars and Active Galactic Nuclei Selected in The Mid-Infrared from Two Spitzer Space Telescope Wide-Area Surveys, The Astronomical Journal, 133:186-205.

Lacy, M., Ridgway, S. E., Sajina, A., et al. 2015. The Spitzer Mid-Infrared AGN Survey. Ii. The Demographics and Cosmic Evolution of The AGN Population, The Astrophysical Journal, 802:102.

Lacy, M., Storrie-Lombardi, L. J., Sajina, A., et al. 2004. Obscured and Unobscured Active Galactic Nuclei in The Spitzer Space Telescope First Look Survey, The Astrophysical Journal Supplement Series, 154:166–169.

Magorrian, J., Tremaine, S., Richstone, D., et al. 1998. The Demography of Massive Dark Objects in Galaxy Centers, The Astronomical Journal, 115:2285-2305.

Martínez-Sansigre, A., Rawlings, S., Lacy, M., et al. 2005. The Obscuration by Dust of Most of the Growth of Supermassive Black Holes, Nature, 436: 666–669.

Mushotzky, R. 2004, in Astrophysics and Space Science Library, Vol. 308, Supermassive Black Holes in The Distant Universe, ed. A. J. Barger, 53.

Mushotzky, R. F., Done, C., & Pounds, K. 1993. X-ray Spectra and Time Variability of Active Galactic Nuclei, The Annual Review of Astronomy and Astrophysics, 31:717-717.

Neugebauer G., Oke J. B., Becklin E. E., Mathews K., 1979. Absolute Spectral Energy Distribution of Quasi-stellar Objects Ffom 0.3 To 10 Microns, The Astrophysical Journal, 230: 79-94.

Polletta, M.D.C., et al. 2006. Chandra and Spitzer Unveil Heavily Obscured Quasars in The Chandra/SWIRE Survey, The Astrophysical Journal, 642:673–693.

Rieke, G. H., & Lebofsky, M. J. 1981. Spectral Components of NGC 4151, The Astrophysical Journal, 250:87-97.

Rosen, S. R., Webb, N. A., Watson, M. G., et al. 2016. The XMM-Newton Serendipitous Survey: VII. The Third XMM-Newton Serendipitous Source Catalogue, Astronomy and Astrophysics, 590, A1.

Sheth, K., Regan, M., Hinz, J. L., et al. 2010. The Spitzer Survey of Stellar Structure in Galaxies (S4G), Publications of The Astronomical Society of the Pacific, 122:1397–1414.

Silk J., Rees M. J., 1998. Quasars and Galaxy formation, Astronomy and Astrophysics, 331, L1-L4.

Steffen A. T., Barger A. J., Cowie L. L., Mushotzky R. F., Yang Y., 2003a. The Changing Active Galactic Nucleus Population, The Astrophysical Journal, 596: L23–L26.

Stern, D., Assef, R. J., Benford, D. J., et al. 2012. Mid-Infrared Selection of Active Galactic Nuclei with The Wide-Field Infrared Survey Explorer. I. Characterizing Wise-Selected Active Galactic Nuclei in Cosmos, The Astrophysical Journal, 753:30.

Stern, D., Eisenhardt, P., Gorjian, V., et al. 2005. Mid-Infrared Selection of Active Galaxies, The Astrophysical Journal, 631:163–168.

Tremaine, S., Gebhardt, K., Bender, R., et al. 2002. The Slope of the Black Hole Mass Versus Velocity Dispersion Correlation, The Astrophysical Journal, 574:740–753.

3XMM-DR5 Catalogue.

http://xmmssc.irap.omp.eu/Catalogue/3XMM-DR5/3XMM_DR5.html

The Chandra Source Catalogue Release 1.1. https://cxc.cfa.harvard.edu/csc1/